

Special Issue

Coordination Booster-Catalyst Assembly: Remote Osmium Outperforming Ruthenium in Boosting Catalytic Activity

Tanmoy Mandal, Vivek Singh, and Joyanta Choudhury*^[a]

Abstract: Presented herein is a set of bimetallic and trimetallic “coordination booster-catalyst” assemblies in which the coordination complexes $[Ru^{II}(\text{terpy})_2]$ and $[Os^{II}(\text{terpy})_2]$ acted as boosters for enhancement of the catalytic activity of $[Ru^{II}(\text{NHC})(\textit{para}\text{-cymene})]$ -based catalytic site. The boosters accelerated the oxidative loss of *para*-cymene from the catalytic site to generate the active catalyst during the oxidation

of alkenes and alkynes into corresponding aldehydes, ketones and diketones. It was found that the boosting efficiency of the $[Os^{II}(\text{terpy})_2]$ units was considerably higher than its congener $[Ru^{II}(\text{terpy})_2]$ unit in these assemblies. Mechanistic studies were conducted to understand this unique improvement.

Introduction

Chemists draw inspiration from Nature’s supramolecularly assembled metalloenzyme architectures to manipulate activity and selectivity of synthetic catalysts. For instance, in line with “allosteric effect”, the tactic of incorporating a controlling unit (Con) near or remote to the catalytic center (Cat) of the same molecular catalyst has been realized to be effective in modulating many catalytic reactions.^[1] In synthetic designer catalyst systems, Cons have not only been used as structural change-induced effectors but also as electronic change-based effectors to the Cats. Important examples of Cons acting as effectors to the Cats via stereo-electronic perturbations include a) chromophores for light-induced control,^[2] b) redox-responsive center for electrochemical control,^[3] c) Lewis acidic moieties for electronic control,^[4] and d) coordination complexes for structural and/or electronic control^[5] etc.. Remarkable effects on the regulation of catalytic activity have been achieved through such approaches. This opens up the possibility of realizing and developing new and unique Con-Cat assemblies (Figure 1 A).

Recently, we reported “ $Ru^{II}(\text{terpy})_2$ - $Ru^{II}(\text{NHC})(\textit{para}\text{-cymene})$ ” and “ $Ru^{II}(\text{terpy})_2$ - $Pd^{II}(\text{NHC})(\text{CH}_3\text{CN})$ ”-based Con-Cat assemblies (terpy = 2,2':6,2''-terpyridine; NHC = *N*-heterocyclic carbene; *p*-cymene = *para*-cymene),^[5] wherein the remotely installed Con unit- “ $Ru^{II}(\text{terpy})_2$ ”- was exploited as a “coordination booster” for enhancing the catalytic efficiency of the “ $Ru(\text{NHC})$ ” and

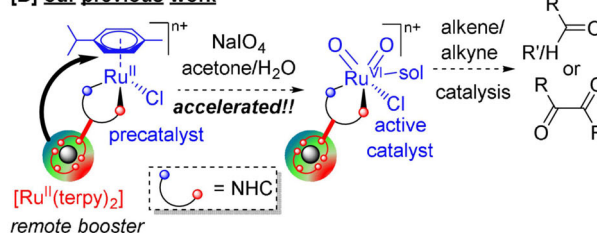
“ $Pd(\text{NHC})$ ” catalytic (Cat) sites in oxidative catalysis. In case of “ $Ru^{II}(\text{terpy})_2$ - $Ru^{II}(\text{NHC})(\textit{para}\text{-cymene})$ ” assembly (Figure 1 B),^[5a] the likely role of this unprecedented remote coordination booster, $Ru^{II}(\text{terpy})_2$, was to act as an electronic-trigger toward accel-

[A] general design of ‘Con-Cat’ assembly



- # Chromophore (light control)
- # Redox-responsive unit (electrochemical control)
- # Lewis acid (electronic control)
- # Coordination complex (stereoelectronic control)

[B] our previous work



[C] this work

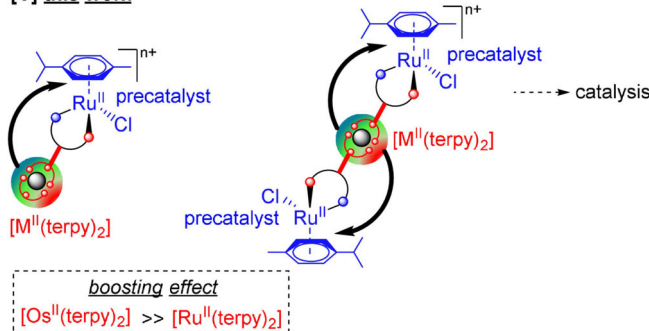


Figure 1. [A] General design of “Con-Cat” assembly. [B] Our previous work on “coordination booster-catalyst” assembly. [C] Key findings of the present work.

[a] T. Mandal, V. Singh, Prof. Dr. J. Choudhury
Organometallics & Smart Materials Laboratory
Department of Chemistry
Indian Institute of Science Education and Research Bhopal
Bhopal 462 066 (India)
E-mail: joyanta@iiserb.ac.in

Supporting information and the ORCID identification number(s) for the author(s) of this article can be found under:
<https://doi.org/10.1002/asia.201901215>.

This manuscript is part of a special issue celebrating the 20th anniversary of the Chemical Research Society of India (CRSI). A link to the Table of Contents of the special issue will appear here when the complete issue is published.

ating the dissociation of the attached labile ligand (*p*-cymene) at the catalytic Ru center and facilitating the generation of the active catalyst (high-valent Ru-oxo species), in the olefin/alkyne oxidation catalysis. Notably, in several catalytic reactions including oxidative catalysis, labilization or dissociation or loss of attached ligands such as η^5 -Cp* and η^6 -arene from pre-catalysts, was found to be crucial for the generation of active catalysts.^[6]

In this work, we demonstrate that the replacement of the remote “coordination booster” Ru^{II}(terpy)₂, with its congener Os^{II}(terpy)₂ unit in such **Con-Cat** assemblies led to considerable enhancement of the boosting effect in oxidative catalysis. Two sets of assemblies of the type “M^{II}(terpy)₂-Ru^{II}(NHC)(*p*-cymene)” (**Con-Cat**) and “Ru^{II}(NHC)(*p*-cymene)-M^{II}(terpy)₂-Ru^{II}(NHC)(*p*-cymene)” (**Cat-Con-Cat**) (where M = Ru and Os) were tested to validate this enhanced boosting effect in the oxidation of alkenes and alkynes to carbonyl compounds (Figure 1C). It is needless to mention that oxidative cleavage of alkenes and alkynes, which leads to form small functional oxygenated derivatives, is utilized in many processes like biomass degradation, synthesis of fine and bulk chemicals etc., thus contributing to both industrial and academic research.^[7]

Results and Discussion

The present study demanded a systematic design of the **Con-Cat** assemblies to probe the boosting effect of “Os^{II}(terpy)₂” in comparison to “Ru^{II}(terpy)₂” in the selected oxidative catalysis. Therefore, with this idea, the (**Con-Cat**) assemblies—[Ru^{II}(terpy)₂-Ru^{II}(NHC)(*p*-cymene)Cl](PF₆)₃ (**Ru_{Con}-Ru_{Cat}**) and [Os^{II}(terpy)₂-Ru^{II}(NHC)(*p*-cymene)Cl](PF₆)₃ (**Os_{Con}-Ru_{Cat}**), and the (**Cat-Con-Cat**) assemblies—[Ru^{II}(NHC)(*p*-cymene)Cl-Ru^{II}(terpy)₂-Ru^{II}(NHC)(*p*-cymene)Cl](PF₆)₄ (**Ru_{cat}-Ru_{Con}-Ru_{Cat}**) and [Ru^{II}(NHC)(*p*-cymene)Cl-Os^{II}(terpy)₂-Ru^{II}(NHC)(*p*-cymene)Cl](PF₆)₄ (**Ru_{cat}-Os_{Con}-Ru_{Cat}**) were employed in this study, in line with our preliminary report on boosting effect of (**Ru_{Con}-Ru_{Cat}**) in comparison to the activity of the model catalyst ^{mod}Ru_{cat} (Figure 2).^[5a] The new systems (**Os_{Con}-Ru_{Cat}**), (**Ru_{cat}-Ru_{Con}-Ru_{Cat}**), and (**Ru_{cat}-Os_{Con}-Ru_{Cat}**) were synthesized in accordance with the procedure used for (**Ru_{Con}-Ru_{Cat}**) and characterized fully by ¹H, ¹³C{¹H}, and 2D NMR spectroscopic, and high-resolution electron-spray ionization mass spectrometric (HR-ESIMS) techniques (for details, see Supporting Information). In ¹H NMR spectra, the absence of the imidazolium NCHN proton, and at the same time, the presence of the characteristic four doublet peaks with the integration of one proton each in the range of 4.5–6.5 ppm, one septet peak at 2.38 ppm with the integration of one proton, and two doublet peaks with the integration of three protons each in the range of 0.86–0.90 ppm suggested the NHC-bound ruthenium-coordinated *para*-cymene backbone in all the complexes. Moreover, the characteristic Ru–C_{NHC} peak appeared at ≈184.5 ppm in ¹³C{¹H} NMR spectra of the complexes.^[8] The HR-ESIMS analyses supported with the expected isotopic patterns confirmed the corresponding bimetallic or trimetallic cations present as the major species in solution. In the UV-vis spectra of **Ru_{Con}-Ru_{Cat}** and **Ru_{cat}-Ru_{Con}-Ru_{Cat}**, the [Ru^{II}(terpy)₂] chromophoric moiety displayed the spin-al-

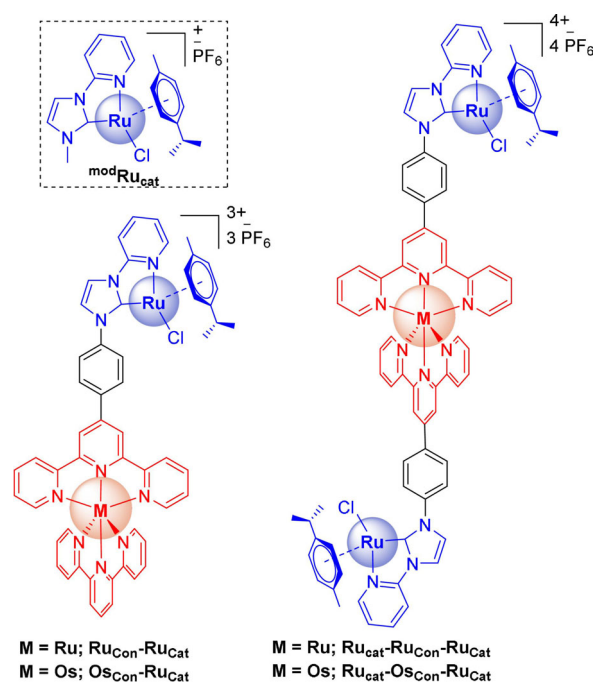


Figure 2. “Con-Cat” and “Cat-Con-Cat” assemblies used in this work. Inset shows the model catalyst ^{mod}Ru_{cat} without having a coordination booster.

lowed ¹MLCT band at ≈491 nm (Figure 3A,B).^[9] On the other hand, for **Os_{Con}-Ru_{Cat}** and **Ru_{cat}-Os_{Con}-Ru_{Cat}**, the [Os^{II}(terpy)₂] moiety exhibited not only the ¹MLCT band at ≈484 nm and ≈492 nm, but also the spin-forbidden ³MLCT band at ≈667 nm and ≈675 nm, respectively, due to large spin-orbit coupling caused by the heavy Os atom (Figure 3A,B).^[9] The electrochemical properties of the redox-active Ru and Os centers in all the complexes were evaluated by differential pulse

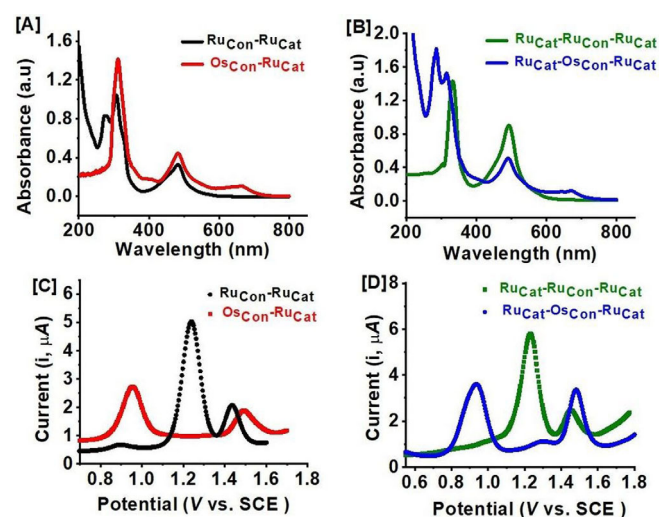


Figure 3. [A], [B] UV-vis absorption spectra (concentration = 0.05 mM in CH₃CN), and [C], [D] DPV plots (concentration = 0.3 mM in CH₃CN, supporting electrolyte = 0.1 M solution of *n*Bu₄NPF₆ in CH₃CN, working electrode = Pt disk (1 mm diameter), counter electrode = a Pt wire, reference electrode = saturated calomel electrode) of the assemblies. Ferrocene (*E*_{1/2}, Fc/Fc⁺ = 0.37 V vs. SCE) was used as an external calibration standard for the DPV experiments.

voltammetric (DPV) measurements. The reversible $\text{Ru}_{\text{Con}}^{\text{II/III}}$ couple of the $\text{Ru}^{\text{II}}(\text{terpy})_2$ unit in $\text{Ru}_{\text{Con}}\text{-Ru}_{\text{Cat}}$ and the $\text{Os}_{\text{Con}}^{\text{II/III}}$ couple of the $\text{Os}^{\text{II}}(\text{terpy})_2$ unit in $\text{Os}_{\text{Con}}\text{-Ru}_{\text{Cat}}$ were characterized at $E_{1/2}$ values of 1.239 V and 0.950 V versus SCE (saturated calomel electrode) respectively (Figure 3C).^[9] In these two systems, the $E_{1/2}$ values of the $\text{Ru}_{\text{Cat}}^{\text{II/III}}$ couple were found to be 1.438 V and 1.490 V versus SCE respectively (Figure 3C).^[8a] Similar $E_{1/2}$ values for the $\text{Ru}_{\text{Con}}^{\text{II/III}}$, $\text{Os}_{\text{Con}}^{\text{II/III}}$, and $\text{Ru}_{\text{Cat}}^{\text{II/III}}$ redox couples were observed in case of the $\text{Ru}_{\text{Cat}}\text{-Ru}_{\text{Con}}\text{-Ru}_{\text{Cat}}$ and $\text{Ru}_{\text{Cat}}\text{-Os}_{\text{Con}}\text{-Ru}_{\text{Cat}}$ assemblies, as well (Figure 3D). It was significant to note that the $E_{1/2}$ values of the catalytic $\text{Ru}_{\text{Cat}}^{\text{II/III}}$ redox center assembled with remote Ru_{Con} in both $\text{Ru}_{\text{Con}}\text{-Ru}_{\text{Cat}}$ and $\text{Ru}_{\text{Cat}}\text{-Ru}_{\text{Con}}\text{-Ru}_{\text{Cat}}$ systems were shifted to more positive potential by ≈ 100 mV as compared to that in the model catalyst $\text{modRu}_{\text{Cat}}$. On the other hand, in case of $\text{Os}_{\text{Con}}\text{-Ru}_{\text{Cat}}$ and $\text{Ru}_{\text{Cat}}\text{-Os}_{\text{Con}}\text{-Ru}_{\text{Cat}}$ assemblies having remote Os_{Con} , the $E_{1/2}(\text{Ru}_{\text{Cat}}^{\text{II/III}})$ values were shifted to more positive potential by ≈ 150 mV as compared to that in the model catalyst $\text{modRu}_{\text{Cat}}$. These data clearly suggested that in the assemblies containing remote Os_{Con} unit, the catalytic Ru_{Cat} center is more electron-deficient than those with the remote Ru_{Con} center.

This disparity had significant influence in the catalytic efficiency of the assemblies. Thus, in a model catalytic oxidation of 4-methylstyrene to 4-methylbenzaldehyde, under identical catalyst loading and reaction conditions, both the Os_{Con} -containing assemblies, $\text{Os}_{\text{Con}}\text{-Ru}_{\text{Cat}}$ and $\text{Ru}_{\text{Cat}}\text{-Os}_{\text{Con}}\text{-Ru}_{\text{Cat}}$ were found to be relative much more active than the corresponding Ru_{Con} -containing assemblies, $\text{Ru}_{\text{Con}}\text{-Ru}_{\text{Cat}}$ and $\text{Ru}_{\text{Cat}}\text{-Ru}_{\text{Con}}\text{-Ru}_{\text{Cat}}$ as shown in Figure 4. An additional activity order of $\text{Ru}_{\text{Con}}\text{-Ru}_{\text{Cat}} > \text{Ru}_{\text{Cat}}\text{-Ru}_{\text{Con}}\text{-Ru}_{\text{Cat}}$ and $\text{Os}_{\text{Con}}\text{-Ru}_{\text{Cat}} > \text{Ru}_{\text{Cat}}\text{-Os}_{\text{Con}}\text{-Ru}_{\text{Cat}}$ was also evident from the kinetic profile of the catalytic reactions. This might be related to the proportionate magnitude of boosting effect of the Ru_{Con} and Os_{Con} units imparted to per catalytic Ru_{Cat} center.

The observed enhanced boosting effect of the Os_{Con} -containing precatalysts in comparison to the Ru_{Con} -containing

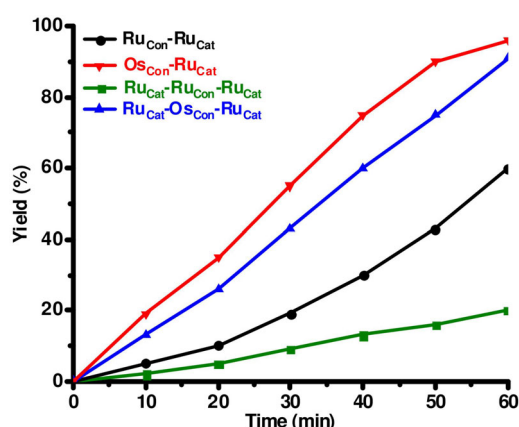


Figure 4. Comparison of catalytic activity of all the precatalysts for oxidation of 4-methylstyrene to 4-methylbenzaldehyde. Reaction conditions: 4-methylstyrene, 0.4 mmol; NaIO_4 , 1.0 mmol; precatalyst, 0.002 mmol for $\text{Ru}_{\text{Con}}\text{-Ru}_{\text{Cat}}$ and $\text{Os}_{\text{Con}}\text{-Ru}_{\text{Cat}}$, 0.001 mmol for $\text{Ru}_{\text{Cat}}\text{-Ru}_{\text{Con}}\text{-Ru}_{\text{Cat}}$ and $\text{Ru}_{\text{Cat}}\text{-Os}_{\text{Con}}\text{-Ru}_{\text{Cat}}$; mesitylene, 0.2 mmol as internal standard; acetone + water (1:1, 6 mL), room temperature.

counterparts could be associated to the relatively faster loss of the attached *para*-cymene ligand from the Ru_{Cat} center in case of the former species, to generate Ru-oxo active catalyst upon oxidative activation during catalysis. Thus, ^1H NMR spectroscopic monitoring showed that the addition of 10 equiv of NaIO_4 to the solutions of $\text{Os}_{\text{Con}}\text{-Ru}_{\text{Cat}}$ and $\text{Ru}_{\text{Cat}}\text{-Os}_{\text{Con}}\text{-Ru}_{\text{Cat}}$ precatalysts resulted in the complete loss of *para*-cymene within just 2 min (Figure 5II,IV). On the other hand, under same conditions, the least active precatalyst, $\text{Ru}_{\text{Cat}}\text{-Ru}_{\text{Con}}\text{-Ru}_{\text{Cat}}$ did not show the complete loss of *para*-cymene even after 30 min (Figure 5III). Notably, the intermediate active precatalyst, $\text{Ru}_{\text{Con}}\text{-Ru}_{\text{Cat}}$ took 5 min for the same, as reported earlier (Figure 5I). The poor resolution of the spectral peaks in the ^1H NMR spectral traces upon addition of NaIO_4 to the precatalysts could be due to the formation of the paramagnetic Ru-oxo species at the Ru_{Cat} sites.

To further probe the effect of the addition of IO_4^- on the Ru_{Cat} as well as the Ru_{Con} and Os_{Con} sites in the representative $\text{Ru}_{\text{Cat}}\text{-Ru}_{\text{Con}}\text{-Ru}_{\text{Cat}}$ and $\text{Ru}_{\text{Cat}}\text{-Os}_{\text{Con}}\text{-Ru}_{\text{Cat}}$ assemblies, DPV studies were conducted. Accordingly, the DPV plots clearly showed the gradual loss of the $\text{Ru}_{\text{Cat}}^{\text{II/III}}$ redox peak and appearance of the expected catalytic current at the potential values corresponding to the Ru_{Cat} site of the precatalysts, whereas the $\text{Ru}_{\text{Con}}^{\text{II/III}}$ and $\text{Os}_{\text{Con}}^{\text{II/III}}$ redox signals remained intact (Figure 6A,B). The fact that the chromophoric Ru_{Con} and Os_{Con} sites in $\text{Ru}_{\text{Cat}}\text{-Ru}_{\text{Con}}\text{-Ru}_{\text{Cat}}$ and $\text{Ru}_{\text{Cat}}\text{-Os}_{\text{Con}}\text{-Ru}_{\text{Cat}}$ precatalysts remained unaffected by the action of the IO_4^- oxidant, even during catalysis, was reconfirmed by UV-vis spectroscopic studies as well (Figure 7A,B).

Next, the most active precatalyst, $\text{Os}_{\text{Con}}\text{-Ru}_{\text{Cat}}$ was subjected to a sub-stoichiometric control reaction with 4-methylstyrene in the presence of NaIO_4 (precatalyst:4-methylstyrene: NaIO_4 ; 1:10:25) in $\text{CH}_3\text{COCH}_3/\text{H}_2\text{O}$ (1:1, v/v) for 5 min at room temperature to assess the species present during the catalysis. The GC analysis of the reaction mixture confirmed the formation of the 4-methylbenzaldehyde product (substrate:product, 1:3). In addition, the ESIMS analysis showed a number of cluster peaks related to different Os-Ru containing species, including the parent complex signatred at $m/z = 646.5899$ for $[\text{C}_{54}\text{H}_{45}\text{N}_9\text{OsRuClPF}_6]^{2+}$ and $m/z = 382.7010$ for $[\text{C}_{54}\text{H}_{45}\text{N}_9\text{OsRuCl}]^{3+}$, as well as other species at $m/z = 369.3636$ for $[\text{C}_{44}\text{H}_{31}\text{N}_9\text{Os}^{\text{II}}\text{Ru}^{\text{II}}(\text{CH}_3\text{COCH}_3)(\text{H}_2\text{O})_2\text{Cl}]^{3+}$ and $m/z = 336.6543$ for $[\text{C}_{44}\text{H}_{31}\text{N}_9\text{Os}^{\text{II}}\text{Ru}^{\text{VI}}\text{-H} + (\text{O})_2]^{3+}$ (for details, see Supporting Information) The presence of the later fragments indicated that the removal of *para*-cymene from the Ru_{Cat} center and the formation of dioxo ruthenium(VI) species were necessary steps during the catalysis. Notably, when a solution of the precatalyst $\text{Os}_{\text{Con}}\text{-Ru}_{\text{Cat}}$ in $\text{CH}_3\text{COCH}_3/\text{H}_2\text{O}$ (4:1, v/v) in the absence of NaIO_4 was subjected to ESIMS analysis, no such peaks corresponding to the removal of *para*-cymene and the formation of dioxo ruthenium(VI) species were detected.

Lastly, to assess the rate-determining step of this oxidation reaction, order dependencies on the precatalyst, oxidant and substrate were determined via initial rate kinetics method. It showed approximately first-order dependencies on the precatalyst and oxidant, and zero-order dependency on the substrate (see Supporting Information). This study suggested that

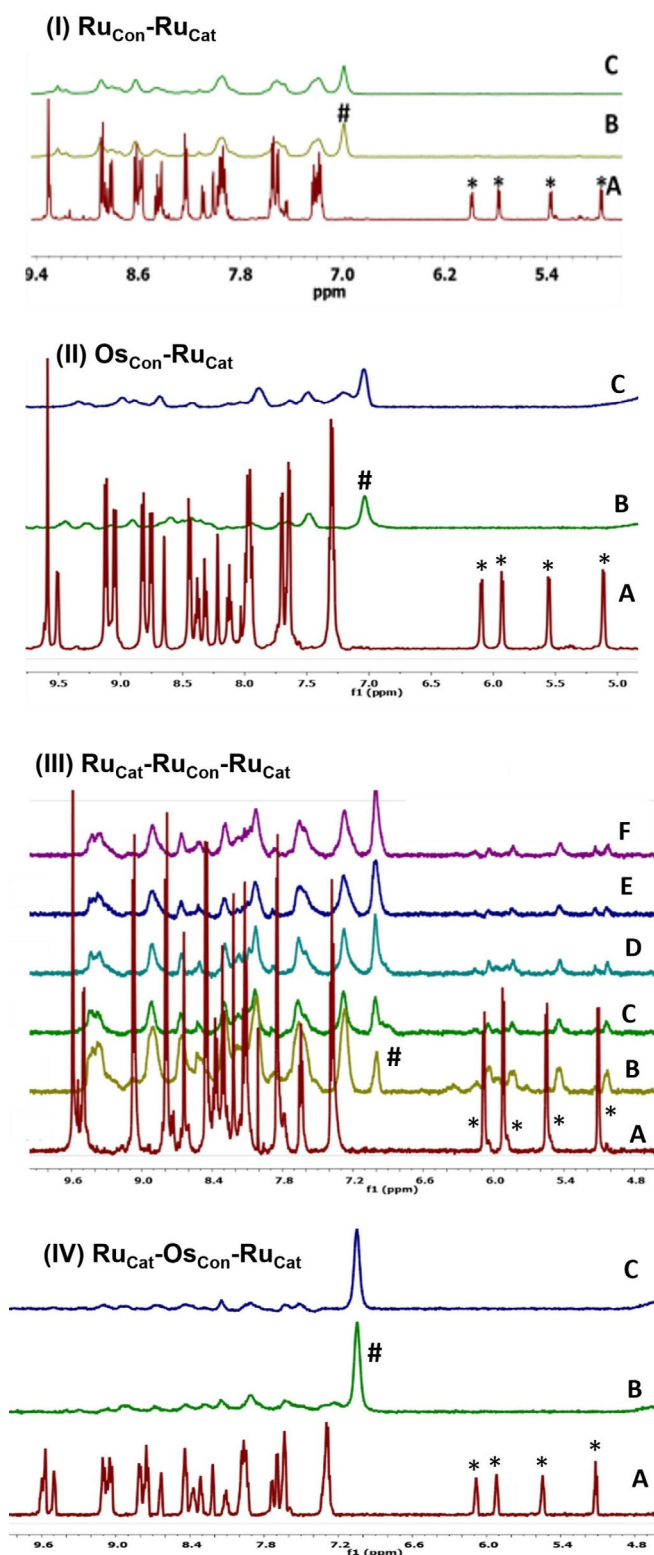


Figure 5. ^1H NMR studies of the assemblies in presence of 10 equiv of NaIO_4 ($[\text{D}_6]\text{acetone-d}_2\text{O}$; 3:2). * = resonance peaks related to ruthenium coordinated *para*-cymene. # = resonance peaks related to free *para*-cymene. (I) For $\text{Ru}_{\text{Con}}\text{-Ru}_{\text{Cat}}$: A = only complex, B = 5 min (after addition of NaIO_4), C = 10 min; (II) For $\text{Os}_{\text{Con}}\text{-Ru}_{\text{Cat}}$: A = only complex, B = 2 min (after addition of NaIO_4), C = 5 min; (III) For $\text{Ru}_{\text{Cat}}\text{-Ru}_{\text{Con}}\text{-Ru}_{\text{Cat}}$: A = only complex, B = 2 min (after addition of NaIO_4), C = 5 min, D = 10 min, E = 20 min, F = 30 min; (IV) For $\text{Ru}_{\text{Cat}}\text{-Os}_{\text{Con}}\text{-Ru}_{\text{Cat}}$: A = only complex, B = 2 min (after addition of NaIO_4), C = 5 min.

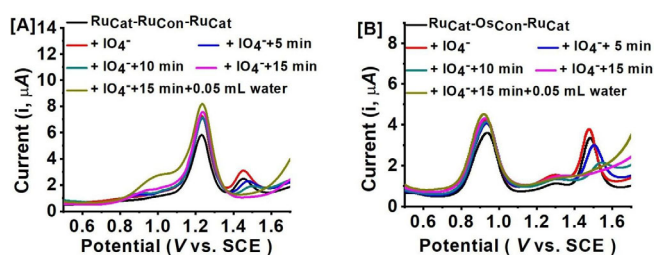


Figure 6. DPV studies of (A) $\text{Ru}_{\text{Cat}}\text{-Ru}_{\text{Con}}\text{-Ru}_{\text{Cat}}$ and (B) $\text{Ru}_{\text{Cat}}\text{-Os}_{\text{Con}}\text{-Ru}_{\text{Cat}}$ assemblies in presence of 20 equiv of $n\text{Bu}_4\text{NIO}_4$ in CH_3CN .

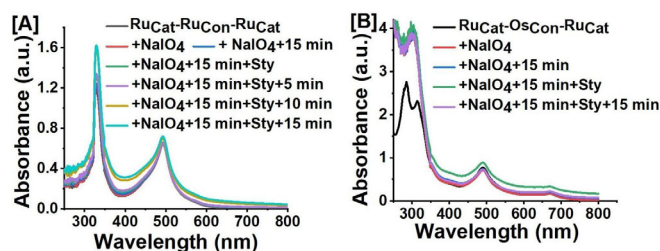


Figure 7. UV-vis absorption spectroscopic studies of (A) $\text{Ru}_{\text{Cat}}\text{-Ru}_{\text{Con}}\text{-Ru}_{\text{Cat}}$ and (B) $\text{Ru}_{\text{Cat}}\text{-Os}_{\text{Con}}\text{-Ru}_{\text{Cat}}$ assemblies in presence of 100 equiv of aqueous NaIO_4 followed by 100 equiv of styrene in acetone.

the rate-determining step might involve a reaction of the pre-catalyst and NaIO_4 to generate the active dioxo-species, and might not involve the substrate. The Hammett study on the substrate resulted in near-zero (0.0057) ρ value, and thus showed that the electronic effect of the substrate had no effect on the rate of the reaction (see Supporting Information), supporting the above proposition.

Based on all of the above studies, the most active precatalyst, $\text{Os}_{\text{Con}}\text{-Ru}_{\text{Cat}}$ was utilized for oxidation of alkenes and alkynes to the corresponding carbonyl products as summarized in Table 1. A similar activity of $\text{Os}_{\text{Con}}\text{-Ru}_{\text{Cat}}$ observed under both normal and dark conditions suggested that the remote $\text{Os}^{\text{II}}(\text{terpy})_2$ unit in the assembly did not act as a photo-trigger during the catalysis. Moreover, the corresponding NHC precursor of the precatalyst $\text{Os}_{\text{Con}}\text{-Ru}_{\text{Cat}}$ devoid of the catalytic unit " $\text{Ru}^{\text{II}}(\text{NHC})(p\text{-cymene})$ ", did not show any catalytic activity under similar conditions, as expected. Interestingly, this catalyst was found to be inactive toward the oxidation of the CH_3 group in 4-methylstyrene (or in 4-methylbenzaldehyde) (entry 2, Table 1). In our earlier studies also,^[10] we found that this kind of Ru-NHC-based catalysts could oxidize the methylene C–H bonds such as $-\text{CH}_2-$ (as in ethylbenzene), but not methyl C–H bonds, such as $-\text{CH}_3$ (as in toluene). $\text{Os}_{\text{Con}}\text{-Ru}_{\text{Cat}}$ was further applied for selective oxidation of styryl double bond in the presence of several oxidation-sensitive functional groups as present in some selected substrates (Figure 8). Interestingly, only styryl double bond was converted to the corresponding aldehyde functionality under the given reaction conditions, without affecting the other oxidation-sensitive functional groups such as aliphatic olefins—both internal and terminal, benzylic C–H bonds and aromatic alkynes. The aldehyde products were isolated in good yields, in all cases. Notably, the

Table 1. Examples of alkene/alkyne oxidation catalysis with $\text{Os}_{\text{con}}\text{-Ru}_{\text{cat}}$ [a]

#	Substrate	Product	Yield [%]/ Time [min]
1	Styrene (1 a)	Benzaldehyde (3 a)	90/40
2	4-Methylstyrene (1 b)	4-Methylbenzaldehyde (3 b)	80/40
3	4-Chlorostyrene (1 c)	4-Chlorobenzaldehyde (3 c)	85/40
4	4-Fluorostyrene (1 d)	4-Fluorobenzaldehyde (3 d)	76/40
5	α -Methyl styrene (1 e)	Acetophenone (3 e)	50/200
6	4-Vinylanisole (1 f)	4-Methoxybenzaldehyde (3 f)	66/60
7	4-Bromostyrene (1 g)	4-Bromobenzaldehyde (3 g)	86/40
8	<i>trans</i> -Stilbene (1 h)	Benzaldehyde (3 h)	87/40
9	<i>cis</i> -Stilbene (1 i)	Benzaldehyde (3 i)	90/40
10	Allylbenzene (1 j)	2-Phenylacetaldehyde (3 j)	72/40
11	Diphenylacetylene (2 a)	Benzil (4 a)	85/40
12	Bis(4-methoxyphenyl)acetylene (2 b)	4,4'-Dimethoxybenzil (4 b)	80/180
13	1-Phenyl-1-butyne (2 c)	1-phenylbutane-1,2-dione (4 c)	73/180

[a] Reaction conditions: substrate, 0.4 mmol, NaIO_4 (1.0 mmol), $\text{Os}_{\text{con}}\text{-Ru}_{\text{cat}}$ (0.5 mol%), acetone + water (1:1, v/v, 6 mL), room temperature. The yields of the products were calculated by calibrated GC analysis. Separate calibration curves were used for different classes of products to take care of different GC response factors.

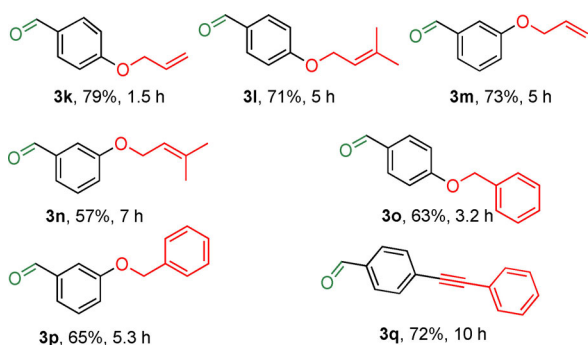


Figure 8. Selective oxidation of styryl bonds in presence of other oxidation-sensitive functionalities (shown in red color) by $\text{Os}_{\text{con}}\text{-Ru}_{\text{cat}}$. Reaction conditions: substrate, 0.4 mmol, NaIO_4 (1.0 mmol), $\text{Os}_{\text{con}}\text{-Ru}_{\text{cat}}$ (0.5 mol%), acetone + water (1:1, v/v, 6 mL), room temperature. The yields of the products were expressed as isolated yields after purification by column chromatography.

alkyne functionality in product **3 q** (Figure 8) remained intact under the applied conditions; but it could be converted to the corresponding diketone **4 d** upon further treating with additional 2.5 equiv of NaIO_4 in the presence of the catalyst (see Supporting Information).

Conclusion

In summary, this work demonstrated that the boosting effect of covalently attached remote coordination complex, “ $\text{M}^{\text{II}}(\text{terpy})_2$ ” in “coordination booster-catalyst” assemblies toward activity of the $[\text{Ru}^{\text{II}}(\text{NHC})(\textit{para}\text{-cymene})]$ -based catalytic center could be enhanced by replacing $\text{Ru}^{\text{II}}(\text{terpy})_2$ with $\text{Os}^{\text{II}}(\text{terpy})_2$ unit. Mechanistic studies with the help of NMR spectroscopy, electrochemical analysis and UV/Vis absorption spectroscopy suggested that the boosting effect was correlated to an accelerated *para*-cymene loss from the precatalyst site to generate active catalyst in case of $\text{Os}^{\text{II}}(\text{terpy})_2$ -containing assemblies. The most effective catalyst was utilized in the selective oxidation of several styrene-type substrates.

Experimental Section

General procedure for catalytic oxidation of alkenes and alkynes

Comparison of catalytic activity of all the catalysts as well as selective oxidation of styrene derivatives were performed in aqueous acetone medium. Substrate (0.4 mmol), catalyst (0.5 mol% for bimetallic and 0.025 mol% for trimetallic systems), and mesitylene as an internal standard (0.2 mmol) in acetone (1 mL) were taken in a 10 mL round bottom flask. Next, 2 mL of acetone and 2 mL of H_2O were added to it. NaIO_4 (1.0 mmol) was dissolved in 1 mL of H_2O and was transferred to the reaction mixture. The reaction was conducted at room temperature. The formation of product was monitored by GC. After completion of the reaction, the mixture was extracted with ethyl acetate. Evaporation of the solvent furnished the crude product, which was further purified by column chromatography.

Acknowledgements

This work was financially supported by DST-SERB (grant no. EMR/2016/003002) and IISER Bhopal. T.M. thanks CSIR for doctoral fellowship and V.S. thanks IISER Bhopal for MS fellowship. We thank Dr. Suraj K. Gupta for help.

Conflict of interest

The authors declare no conflict of interest.

Keywords: alkenes · coordination assembly · osmium · oxidation · ruthenium

- [1] For representative examples, see: a) A. M. Lifschitz, R. M. Young, J. Mendez-Arroyo, C. M. McGuirk, M. R. Wasielewski, C. A. Mirkin, *Inorg. Chem.* **2016**, *55*, 8301; b) H. J. Yoon, J. Kuwabara, J.-H. Kim, C. A. Mirkin, *Science* **2010**, *330*, 66; c) G. Y. Tonga, Y. Jeong, B. Duncan, T. Mizuhara, R. Mout, R. Das, S. T. Kim, Y.-C. Yeh, B. Yan, S. Hou, V. M. Rotello, *Nat. Chem.* **2015**, *7*, 597.
- [2] For selected references, see: a) K. L. Mulfort, L. M. Utschig, *Acc. Chem. Res.* **2016**, *49*, 835; b) M. R. Norris, J. J. Concepcion, Z. Fang, J. L. Templeton, T. J. Meyer, *Angew. Chem. Int. Ed.* **2013**, *52*, 13580; *Angew. Chem.* **2013**, *125*, 13825; c) D. Chao, M. Zhao, *ChemSusChem* **2017**, *10*, 3358.

- [3] For selected examples, see: a) J. Wei, P. L. Diaconescu, *Acc. Chem. Res.* **2019**, *52*, 415; b) P. Veit, C. Volkert, C. Förster, V. Ksenofontov, S. Schlicher, M. Bauer, K. Heinze, *Chem. Commun.* **2019**, *55*, 4615; c) A. J. Tretor, D. N. Lastovickova, C. W. Bielawski, *Chem. Rev.* **2016**, *116*, 1969; d) S. Klenk, S. Rupf, L. Suntrup, M. van der Meer, B. Sarkar, *Organometallics* **2017**, *36*, 2026; e) A. Feyrer, M. K. Armbruster, K. Fink, F. Breher, *Chem. Eur. J.* **2017**, *23*, 7402; f) S. Ibáñez, M. Poyatos, L. N. Dawe, D. Gusev, E. Peris, *Organometallics* **2016**, *35*, 2747.
- [4] For selected examples, see: a) A. L. Liberman-Martin, R. G. Bergman, T. D. Tilley, *J. Am. Chem. Soc.* **2013**, *135*, 9612; b) A. L. Liberman-Martin, D. S. Levine, W. Liu, R. G. Bergman, T. D. Tilley, *Organometallics* **2016**, *35*, 1064; c) N. S. Lambic, C. A. Brown, R. D. Sommer, E. A. Ison, *Organometallics* **2017**, *36*, 2042; d) H. Guo, Z. Chen, F. Mei, D. Zhu, H. Xiong, G. Yin, *Chem. Asian J.* **2013**, *8*, 888; e) A. M. Johnson, N. D. Contrella, J. R. Sampson, M. Zheng, R. F. Jordan, *Organometallics* **2017**, *36*, 4990; f) T. Chantarojsiri, J. W. Ziller, J. Y. Yang, *Chem. Sci.* **2018**, *9*, 2567.
- [5] a) S. K. Gupta, J. Choudhury, *Chem. Commun.* **2016**, *52*, 3384; b) M. Mondal, J. Joji, J. Choudhury, *Chem. Commun.* **2017**, *53*, 3185; c) C. M. McQuirk, J. Mendez-Arroyo, A. M. Lifschitz, C. A. Mirkin, *J. Am. Chem. Soc.* **2014**, *136*, 16594.
- [6] a) U. Hintermair, S. W. Sheehan, A. R. Parent, D. H. Ess, D. T. Richens, P. H. Vaccaro, G. W. Brudvig, R. H. Crabtree, *J. Am. Chem. Soc.* **2013**, *135*, 10837; b) J. Takaya, J. F. Hartwig, *J. Am. Chem. Soc.* **2005**, *127*, 5756; c) A. B. Chaplin, P. J. Dyson, *J. Organomet. Chem.* **2011**, *696*, 2485; d) M. Otsuka, H. Yokoyama, K. Endob, T. Shibata, *Org. Biomol. Chem.* **2012**, *10*, 3815.
- [7] a) T. Punniyamurthy, S. Velusamy, J. Iqbal, *Chem. Rev.* **2005**, *105*, 2329; b) S. Rup, M. Sindt, N. Oget, *Tetrahedron Lett.* **2010**, *51*, 3123; c) X. Liu, W. Chen, *Organometallics* **2012**, *31*, 6614; d) S. L.-F. Chan, Y.-H. Kan, K.-L. Yip, J.-S. Huang, C.-M. Che, *Coord. Chem. Rev.* **2011**, *255*, 899; e) D. G. Lee, T. Chen, *Comprehensive Organic Synthesis*, Pergamon, Oxford, **1991**; f) R. C. Larock, *Comprehensive Organic Transformations*, Wiley-VCH, New York, **1999**; g) S. Caron, R. W. Dugger, S. G. Ruggeri, J. A. Ragan, D. H. B. Rippin, *Chem. Rev.* **2006**, *106*, 2943; h) S. C. Van Ornum, R. M. Champeau, R. Pariza, *Chem. Rev.* **2006**, *106*, 2990.
- [8] a) S. K. Gupta, S. K. Sahoo, J. Choudhury, *Organometallics* **2016**, *35*, 2462; b) D. Schleicher, H. Leopold, H. Borrmann, T. Strassner, *Inorg. Chem.* **2017**, *56*, 7217; c) F. E. Fernández, M. C. Puerta, P. Valerga, *Organometallics* **2012**, *31*, 6868.
- [9] J. P. Sauvage, J. P. Collin, J. C. Chambron, S. Guillerez, C. Coudret, V. Balzani, F. Barigelli, L. D. Cola, L. Flamigni, *Chem. Rev.* **1994**, *94*, 993.
- [10] S. K. Gupta, J. Choudhury, *ChemCatChem* **2017**, *9*, 1979.

Manuscript received: August 28, 2019

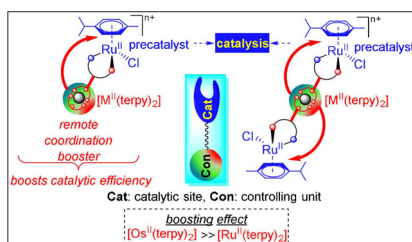
Revised manuscript received: September 26, 2019

Accepted manuscript online: September 27, 2019

Version of record online: ■■■■■, 0000

FULL PAPER

Designer outfit: In the designer “coordination booster-catalyst” assemblies, the remote coordination complexes $[\text{Ru}^{\text{II}}(\text{terpy})_2]$ and $[\text{Os}^{\text{II}}(\text{terpy})_2]$ act as boosters for the enhancement of the catalytic activity of $[\text{Ru}^{\text{II}}(\text{NHC})(\text{para-cymene})]$ -based catalytic site. $[\text{Os}^{\text{II}}(\text{terpy})_2]$ unit boosts more efficiently than its congener $[\text{Ru}^{\text{II}}(\text{terpy})_2]$ unit in these assemblies.



Tanmoy Mandal, Vivek Singh,
Joyanta Choudhury*



**Coordination Booster-Catalyst
Assembly: Remote Osmium
Outperforming Ruthenium in Boosting
Catalytic Activity**

